AVAR-Net: A Lightweight Audio-Visual Anomaly Recognition Framework with a Benchmark Dataset

Amjid Ali[a], Zulfiqar Ahmad Khan[b], Altaf Hussain[a], Muhammad Munsif[a], Adnan Hussain[a], Sung Wook Baik[a,*]

[a]*Sejong University, Seoul, 143-747, Republic of Korea*
[b]*Umeå University, Department of Computer Science, Sweden*

Abstract

Anomaly recognition plays a vital role in surveillance, transportation, healthcare, and public safety. However, most existing approaches rely solely on visual data, making them unreliable under challenging conditions such as occlusion, low illumination, and adverse weather. Moreover, the absence of large-scale synchronized audio-visual datasets has hindered progress in multimodal anomaly recognition. To address these limitations, this study presents AVAR-Net, a lightweight and efficient audio-visual anomaly recognition framework designed for real-world environments. AVAR-Net consists of four main modules: an audio feature extractor, a video feature extractor, fusion strategy, and a sequential pattern learning network that models cross-modal relationships for anomaly recognition. Specifically, the Wav2Vec2 model extracts robust temporal features from raw audio, while MobileViT captures both local and global visual representations from video frames. An early fusion mechanism combines these modalities, and a Multi-Stage Temporal Convolutional Network (MTCN) model that learns long-range temporal dependencies within the fused representation, enabling robust spatiotemporal reasoning. A novel Visual-Audio Anomaly Recognition (VAAR) dataset, is also introduced, serving as a medium-scale benchmark containing 3,000 real-world videos with synchronized audio across ten diverse anomaly classes. Experimental evaluations demonstrate that AVAR-Net achieves 89.29% accuracy on VAAR and 88.56% Average Precision on the XD-Violence dataset, improving Average Precision by 2.8% over existing state-of-the-art methods. These results highlight the effectiveness, efficiency, and generalization capability of the proposed framework, as well as the utility of VAAR as a benchmark for advancing multimodal anomaly recognition research.

*Corresponding author: Sung Wook Baik (email: sbaik3797p@gmail.com)

Keywords: Anomaly Recognition, Visual-Audio, Computer Vision, Video Surveillance, Multimodal Learning

1. Introduction

Anomaly recognition systems are designed to detect patterns or behaviors that deviate from normal activity. They play a critical role in safeguarding people and property, particularly in safety-critical environments [1]. Recent advancements in surveillance systems have increased the focus on anomaly detection, which supports early warnings for threats such as intrusions, violent acts, and other suspicious activities. However, surveillance systems generate vast amounts of data, making manual analysis difficult and resource-intensive. To enhance robustness, recent research has explored audio-visual learning, where one modality can compensate when the other is compromised. However, most surveillance cameras lack audio recording capabilities, leading many studies to focus solely on visual data and overlook the benefits of audio signals [2]. Audio-visual learning has shown significant improvements in multimodal tasks such as event localization [3], audio-visual video parsing [4] Audio-visual separation achieved significantly better results compared to unimodal approaches. Combining both modalities provides clear advantages: visual cues help detect the type and timing of violent acts, while audio signals offer complementary context, especially in visually complex or obstructed scenes. Audio can also penetrate barriers and still be captured by recording devices [5]. Despite these benefits, audio-visual approaches remain underexplored due to the limited availability of diverse and high-quality datasets. The existing datasets in the anomaly detection include XD-Violence [6], CCTV-Fights [7], UCF-Crime [8], CUHK Avenue [9], ShanghaiTech [10], UCSD Pedestrian [11] and RWF-2000 [12], VSD [13], and Shade [14]. Many of these datasets, such as XD-Violence and CCTV-Fights, are restricted to binary classification (normal/abnormal). Others, including UCF-Crime, CUHK Avenue, ShanghaiTech, UCSD Pedestrian, and RWF-2000, lack synchronized audio streams, restricting their suitability for audio-visual research. Although datasets like VSD and Shade provide both audio and visual modalities, they are based on synthetic media and have limited accessibility, reducing their usefulness for real-world benchmarking. This lack of dual-modality datasets hinders advancements in anomaly recognition, highlighting the need for further research and the development of real-world multimodal surveillance systems. Consequently, most prior works focus on unimodal solutions. For example, W. Ullah et al. [15] proposed a two-stream neural network for anomaly detection using the UFC-Crime dataset, relying solely on visual features. Similarly, Perez et al. [9] applied CNNs and motion features to

short clips, which restricts generalization to continuous real-world footage. Additionally, other video-based anomaly detection methods that rely on visual data often struggle in challenging environments like low lighting conditions or obstructed views [13]. In contrast, some studies have explored audio-based anomaly detection for anomaly recognition [16]. Audio-based methods face their own limitations, such as background noise, distortion, and microphone placement [17]. However, combining both modalities improves precision, especially when one is degraded by environmental conditions. Despite this, only a few works have examined audio-visual anomaly recognition. AU Rehman et al. [18] proposed a multimodal anomaly detection method combining audio and visual features for improved surveillance performance. Similarly, Wu et al. [19] introduced a three-branch neural network capturing global, local, and score-based relationships for anomaly detection, though it only performs binary classification without identifying anomaly types. These methods, while multimodal, typically address binary detection without classifying the type of anomaly, limiting real-time applicability. This lack of real-world, synchronized audio-visual datasets has limited progress in developing and benchmarking reliable anomaly recognition models, highlighting the need for new data and methods.

1.1. Research Gaps

Despite increasing interest in surveillance-based anomaly recognition, several key limitations still impede the development of accurate and scalable systems.

- Mostly, the existing anomaly recognition datasets, such as CCTV-Fights, UCF-Crime, CUHK Avenue, and Shanghai Tech, are unimodal, containing either video or audio, but not both. This severely restricts the development and benchmarking of audio-visual systems [19]. Even when both modalities are present, datasets are usually designed for binary detection (normal vs. abnormal) rather than multi-class recognition. Furthermore, many multimodal datasets are derived from non-surveillance domains like movies or games, limiting their relevance for real-world deployment.

- Many existing method, such as [20, 21] , rely on computationally expensive architectures such as 3D-CNNs and Seq2Seq models. These scale poorly with video length, making them unsuitable for real-time anomaly recognition. On the audio set, most approaches depend on handcrafted features such as Mel spectrograms, MFCCs, or zero-crossing rate [22], which are limited in capturing complex temporal dynamics. This restricts their ability to deliver fast and accurate recognition in time-sensitive surveillance contexts.

- Most audio-visual anomaly studies still focus on binary detection and depend on synthetic or entertainment-based datasets. These settings fail to capture the complexities of real surveillance environments, such as occlusion, varying lighting, or multiple overlapping events. As a result, many existing methods fail to generalize and are unsuitable for real-time deployment.

1.2. Contributions

To address the limitations of current audio-visual anomaly recognition systems, this work makes both dataset and model contributions, summarized as follows:

- **A New Benchmark Dataset VAAR:** The study introduces the Visual-Audio Anomaly Recognition (VAAR) dataset, a medium-scale benchmark comprising 3,000 videos with synchronized audio across 10 diverse anomaly classes. The dataset captures complex real-world scenes with rich dynamic and contextual cues, making it suitable for developing and evaluating real-time audio-visual anomaly recognition systems. Compared to existing datasets, VAAR offers greater diversity, realism, and modality alignment.

- **A Novel Audio-Visual Framework AVAR-Net:** The study proposes AVAR-Net, a multimodal anomaly recognition framework that effectively integrates both audio and visual modalities. It leverages a pre-trained MobileViT backbone to capture local and global spatial features from video frames, and Wav2Vec2 to extract robust temporal representations from raw audio. An early fusion mechanism and a Multi-Temporal Convolutional Network (MTCN) with attention modules jointly model long-range temporal dependencies in fused features, enabling robust spatiotemporal anomaly recognition.

- **Comprehensive Evaluation:**The proposed framework is evaluated on both the proposed VAAR dataset and the publicly available XD-Violence benchmark. On the VAAR, AVAR-Net achieves 89.29% accuracy in multi-class recognition, and on XD-Violence, it attains 76.68% accuracy with a 2.8% improvement in Average Precision over existing state-of-the-art models. These results validate the effectiveness and generalization of our approach.

2. Related Work

Anomaly recognition in multi-modal systems has progressed toward detecting complex irregularities with higher precision. Research mainly falls into two areas: video anomaly detection and audio-visual anomaly recognition. However, limited

labeled multi-modal data restricts development, leaving auditory anomaly detection comparatively underexplored. Still, this field offers strong potential for self-monitoring, infrastructure protection, and threat detection.

2.1. Existing Datasets

Anomaly detection has gained substantial attention in recent years, leading to the creation of several benchmark datasets. Among the video-based datasets, UCF-Crime introduced by Sultani et al. [23] is one of the largest collections of untrimmed surveillance videos with video-level labels. The UCSD Pedestrian dataset by Mahadevan et al. [5] focuses on detecting anomalies such as bicycles and carts in pedestrian walkways. Similarly, the CUHK Avenue dataset by Lu et al. [24] includes short video clips with frame-level annotations capturing anomalies like running or throwing. The ShanghaiTech dataset proposed by Liu et al. [7] contains videos from various crowded scenes, including activities such as loitering, running, and cycling in restricted areas. Datasets such as CCTV-Fights [9] and RWF-2000 [11] focus on real-world violent activities captured from surveillance footage. While these video datasets have driven substantial progress, they rely solely on visual information, limiting performance in complex scenes with occlusion, poor lighting, or environmental noise. To overcome these limitations, multimodal datasets have been introduced. For instance, XD-Violence by Wu et al. [10] is a large-scale audio-visual dataset containing diverse anomalies such as fights, explosions, and riots in untrimmed videos. The VSD dataset proposed by Demarty et al. [6] combines movies and web videos with frame-level annotations, incorporating both visual and audio for violent detection. More recently, the SHADE dataset, introduced by Gao et al. [14], provides a synthetic audio-visual benchmark designed for crowd anomaly recognition. Although such datasets have advanced research in anomaly detection, they still face challenges in terms of real-time applicability and multi-class anomaly representation. Therefore, there remains a strong need for comprehensive, well-annotated multimodal benchmarks that better reflect real-world anomaly recognition scenarios.

2.2. Video Anomaly Detection (VAD)

VAD methods can be broadly categorized into handcrafted feature-based and deep learning-based approaches. Early studies relied on handcrafted features such as Histogram of Oriented Gradients (HOG), Histogram of Optical Flow (HOF), Scale-Invariant Feature Transform (SIFT), Spatiotemporal Interest Points (STIP), and Violent Flows (ViF) to capture motion and appearance cues. For instance, A Kaur et al. [25] used a bag-of-words model combining SIFT and STIP for fight detection. Although effective in constrained settings, these handcrafted approaches often

struggle to generalize to complex, dynamic scenes. The emergence of deep learning significantly improved anomaly recognition by enabling end-to-end spatiotemporal feature learning. Convolutional Long Short-Term Memory (ConvLSTM) networks [26] demonstrated superior temporal modeling compared to handcrafted methods, and bidirectional ConvLSTM architectures [27] further enhanced performance in aggression detection. Similarly, Peixoto et al. [28] employed dual deep neural networks to extract spatiotemporal features from video sequences, followed by a shallow classifier for violence recognition. Hybrid deep networks have also been applied for detecting violent activities in drone surveillance footage [29].

More recently, weakly supervised learning has become a dominant paradigm in VAD, reducing the need for frame-level annotations. Pereira et al. [30] introduced a Multiple Instance Learning (MIL) framework with sparsity and smoothness constraints to detect anomalous segments in videos. Li et al. [31] extended this idea using a Transformer-based model [32] for sequence learning. Wu et al. [33] proposed VAD-CLIP, integrating visual and textual features through a dual-branch network for weakly supervised detection. Additionally, unsupervised and semi-supervised techniques such as Fuzzy C-Means clustering [34], Dual-Stream Slow Feature Analysis (DSFA) [35], and adversarial learning frameworks like AE-Net [36] have shown promise for improving anomaly localization and robustness in unlabeled scenarios.

2.3. Visual Audio Anomaly Detection

Similar to VAD, audio-visual anomaly detection (AVAD) integrates auditory and visual cues to enhance event understanding and robustness. Early studies primarily relied on handcrafted audio features such as chroma, pitch, zero-crossing rate (ZCR), audio energy, spectrogram, and Mel-Frequency Cepstral Coefficients (MFCC) to identify violent or abnormal events [37, 38]. However, these shallow representations were often sensitive to background noise and lacked semantic alignment with visual context. With the rise of deep learning, researchers began leveraging multimodal feature fusion to improve performance. For example, Owens et al. [39] explored transferring representations from audio to visual domains, while Arandjelovic et al. [40] examined audio-visual correlations in video scenes. Kitller et al. [41] modeled human behavior using separate Hidden Markov Models (HMMs) for audio and video modalities.

Recent approaches have focused on weakly supervised and self-supervised learning, addressing annotation scarcity and improving temporal reasoning. Leng et al. [42] introduced dual-space representation learning (DSRL) that leverages Euclidean and hyperbolic spaces with cross-space attention to enhance feature discrimination. Jungpil Shin et al. [43] developed a multimodal WS-VAD system that fuses RGB,

Table 1: Overview of publicly available datasets used for video-based and audio-visual anomaly recognition.

Dataset	Method	Class	Modality	Resolution	Description
UCSD-P (2010)	GMM	2	Video	227×227	It covers a single scene with low visual complexity. It has two classes: anomaly and normal.
CUHK-A (2013)	Sparse Recon	2	Video	640×360	It is a medium-scale video-based anomaly detection dataset that has scene diversity and short clips.
VSD (2015)	SVM	2	Video and Audio	640x345	It is based on cinematic violence collected from 32 movie scenes with audio and video information.
UCF-Crime (2018)	MIL	14	Video	320×240	It is a video-based anomaly dataset. It covers 14 different anomaly classes.
S-Tech (2018)	U-Net	2	Video	768×1024	It covers narrow anomaly diversity and a binary class. Additionally, it has no audio information.
CCTV-F (2019)	CNN	2	Video	384×216	It has binary detection fights and non-fights. Additionally, the dataset is unsuitable for dual modality.
XD-V (2021)	GNN	6	Video and Audio	640×346	It includes both audio and video. It emphasizes general binary anomaly detection.
Shade (2024)	ResNet-34	8	Video and Audio	1920×1080	It is a synthetic-based dual-modality dataset. It is collected from game scenes.
RWF-2000 (2024)	FGN	2	Video	1280×1080	It is a video based on binary anomaly detection. It covers fighting and non-fighting scenes.
Our (VAAR)	MobileViT, Wav2vec	10	Video and Audio	1280×720	It is a multi-class, real-time, multimodal anomaly dataset with diverse scenarios.

optical flow, and audio features using attention modules. Similarly, Wei-Cheng et al. [44] proposed a self-supervised contrastive learning method that mitigates false negatives via multi-positive cross-modal pairing, while Zhang et al. [45] introduced Adaptive Temporal Modeling (ATM) and Dynamic Erasing (DE) to better capture variable anomaly durations. More advanced frameworks, such as Meng et al.'s Audio-Visual Collaborative Learning (AVCL) [46] and Xu et al.'s Weakly Supervised VAD (WSVAD) [47], incorporate cross-modal attention, discriminative score refinement, and anomaly suppression to improve generalization and fine-grained event localization.

3. Proposed Framework

The section provides a detailed overview of the proposed AVAR-Net framework as illustrated in Figure 1. The AVAR-Net is designed to recognize anomalies in complex surveillance scenarios using audio-visual data. The AVAR-Net consists of four primary components: 1) video features extraction, 2) audio feature extraction, 3) fusion strategy 4) attention-based sequential pattern learning. First, video streams are segmented into frames and processed by a pre-trained MobileViT model. This

Algorithm 1: Pseudocode of the proposed AVAR-Net, detailing input preprocessing, feature extraction, multimodal fusion, temporal modeling, and anomaly scoring.

Input: Input audio and video stream $AV_d \in \{AV_1, AV_2, \ldots, AV_n\}$
Output: Predicted anomaly categories $C_L \in \{C_1, C_2, \ldots, C_n\}$
Pre-Initialization:
Training data: $TD \leftarrow \{AV_{T1}, AV_{T2}, \ldots, AV_{Tn}\}$
Validation data: $VD \leftarrow \{AV_{V1}, AV_{V2}, \ldots, AV_{Vn}\}$
Components of the framework: $[VF, AF, EF, TL] \leftarrow$ LoadModules()
$\varpi \leftarrow$ InitParameters()
Model Training Process:
for $\alpha, \nu \in \{AV_1, AV_2, \ldots, AV_{n-1}\}$ **do**
  while $a, v \neq 0$ **do**
    $F_\delta \leftarrow VF(\nu)$
    $F_\partial \leftarrow AF(\alpha)$
    $C_{\text{fusion}} \leftarrow EF(F_\delta \oplus F_\partial)$
    if $Length(C_{fusion}) = T(10)$ **then**
      $f_T \leftarrow TL(C_{\text{fusion}})$
      $C_L \leftarrow \text{SoftMax}(FC(f_T))$
Save(ϖ)
Model Testing Process:
Test video data: $TD \leftarrow \{AV_1, AV_2, \ldots, AV_n\}$
Components of the framework: $[VF, AF, EF, TL] \leftarrow$ LoadModules()
Loaded learned parameters: $\varpi \leftarrow$ Load()
for $\alpha, \nu \in \{AV_1, AV_2, \ldots, AV_{n-1}\}$ **do**
  while $d \neq 0$ **do**
    $[F_\delta, F_\partial] \leftarrow [VF(\nu), AF(\alpha)]$
    $C_{\text{fusion}} \leftarrow EF(F_\delta \oplus F_\partial)$
    $f_T \leftarrow TL(C_{\text{fusion}})$
    $C_L \leftarrow \text{SoftMax}(FC(f_T))$

backbone was selected for its ability to combine local spatial encoding using a convolutional neural network (CNN) and global context modelling using Transformer-based attention, making it both efficient and effective for spatial cues in surveillance footage. Compared to heavier architectures like I3D or pure ViT, MobileViT offers faster inference and lower computational overhead while maintaining competitive

accuracy. Secondly, for the audio modality, we employ Wav2Vec2, a self-supervised model trained in large-scale audio corpora. Unlike traditional handcrafted features (e.g., MFCC, spectrograms), Wav2Vec2 learns context-rich, high-resolution audio representations directly from raw waveforms, making it robust to background noise and variable recording conditions common in real-world environments. This model integrates convolutional neural networks and Transformers to effectively model temporal dynamics in the audio signal. The extracted visual and audio features are fused using an early fusion. This approach allows the model to learn joint representations from the start, encouraging alignment between modalities and capturing complementary cues. To model temporal dependencies, AVAR-Net employs an MTCN to capture multi-scale temporal features. MTCN enables parallel computation, better handles long-range dependencies, and scales more efficiently with sequence length. The attention module further helps the model focus on salient temporal segments, improving anomaly recognition. A pseudocode representation of AVAR-Net is provided in Algorithm 1 to illustrate the workflow. Furthermore, to support training and evaluation, A novel audio-visual anomaly recognition dataset was developed covering a diverse range of real-world events. A detailed description of this dataset is provided in Section 3.1.

3.1. Dataset Curation

As shown in table 1, audio-visual datasets for anomaly recognition are often limited in scope and fail to reflect the complexity of real-world scenarios. To address this, VAAR dataset designed to cover a wide range of real-world scenes and events. The dataset was constructed in three stages, with dedicated teams responsible for quality control at each step. First, Team 1 gathered approximately 4000 raw videos from diverse online platforms, including YouTube, Google, TikTok, Twitter (X), Facebook, and news platforms. Next, Team 2 performed temporal segmentation using Bandicut software dividing the videos into meaningful clips based on event boundaries. Finally, Team 3 reviewed and refined to ensure labeling consistency and accuracy. The final dataset consists of 3,000 video clips, each ranging from 5 seconds to 2 minutes in duration. The dataset covers 10 anomaly classes: abuse, baby cry, crash, brawling, explosion, intruder, normal, pain, police siren, and vandalism. These categories were chosen for their relevance to public safety and security-critical applications, as well as their relative underrepresentation in multimodal research. Notably, the selected classes encompass most of the major categories found in existing anomaly detection datasets, while also introducing previously overlooked scenarios, ensuring broader class coverage. Approximately 80% of the videos originate from surveillance footage, while the remaining 20% are drawn from varied sources, including movies

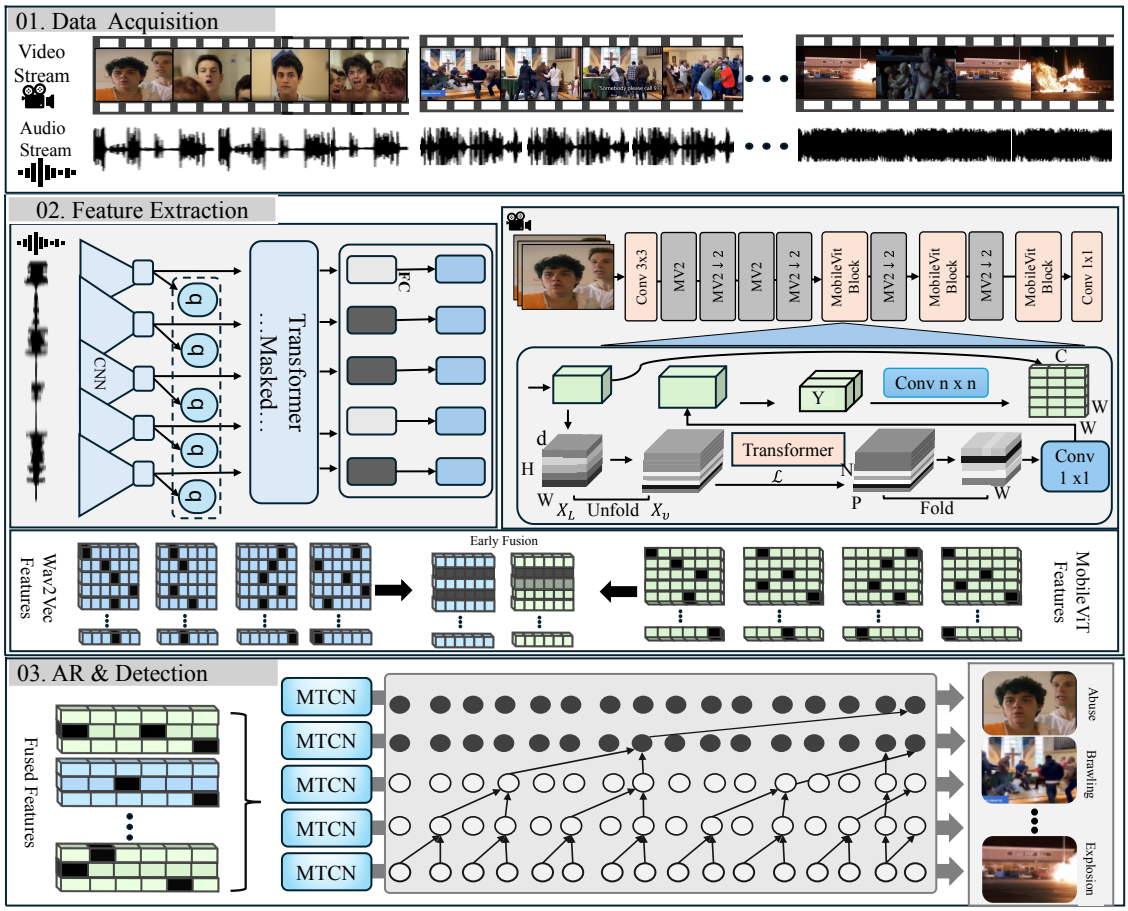

Figure 1: Visual representation of the proposed framework for anomaly recognition, which consists of three core components. The first one is data acquisition, the second is feature extraction, where audio features are extracted using the Wav2Vec2 model, and video features are extracted by MobileViT. Finally, for sequence learning, the Temporal Attention-based MTCN model is used in anomaly recognition.

and user-generated content. This ensures a balanced mix of structured and unstructured environments, enhancing the dataset's applicability across different deployment settings. All videos used in the VAAR dataset were publicly available and are utilized strictly for academic research purposes under fair use guidelines. No private or personally identifiable data were collected or disclosed.

3.2. Video Feature Extractor

To extract video features efficiently while maintaining computational cost, we employ the MobileViT model, which combines convolutional layers and transformers

to capture both local and global features. MobileViT consists of three sub-modules: local feature encoding, global feature encoding, and feature fusion. These modules are responsible for extracting local or global features from the frame. First, the video is processed to extract frames from the anomaly video; then, these frames, with the shape of $X \in \mathbb{R}^{H \times W \times C}$ (where $\mathbb{R}$ represents a set of real numbers, X is a three-dimensional tensor with dimension H, representing the height, W representing the width, and C representing channels) are fed to the Local Feature encoding module, where local features are extracted using standard $N \times N$ convolution ($N = 3$) and 1×1 convolution to adjust the number of channels. The resulting feature tensor is then projected into the Global Representation module in a high-dimensional space $X_L \in \mathbb{R}^{H \times W \times d}$ (where d is the dimension and $d > C$). The global representation module follows the conventional three-step process of unfolding, local processing, and folding, but replaces global processing with local processing using transformers to expand the receptive field. The unfolding and folding processes are similar to those in regular convolution. Subsequently, X_{Unfold} is input into L-stacked Transformers for global information encoding. The inter-column pixel attention is calculated using the attention mechanism to obtain $X_G \in \mathbb{R}^{P \times W \times d}$ (where $P = h \times w$ is the number of pixels in the patch with height h and width w). Finally, the Fold operation is utilized to generate $X_F \in \mathbb{R}^{H \times W \times d}$, which preserves the dimensions of X_L. The Transformer's output enables the receptive field to expand to $H \times W$, as each pixel in the output incorporates information from every pixel in the input feature map, as given in Eq 1.

$$X_G(p) = \text{Transformer}(X_{\text{Unfold}}(p)), \quad 1 \leq p \leq P \tag{1}$$

The module then resizes the number of channels to its original size, resulting in $X \in \mathbb{R}^{H \times W \times C}$ with dimensions matching the initial input X. Next, the skip connection combines the original input X with the transformed features via concatenation, giving $X \in \mathbb{R}^{H \times W \times 2C}$. The output $Y \in \mathbb{R}^{H \times W \times C}$ is derived using a convolution layer with a kernel size of $n \times n$ (where $n = 3$) for feature fusion. Compared to traditional convolution modules, the proposed extractor more effectively captures both local and global information. The integrated Transformer retains positional context, enabling efficient feature learning with fewer layers.

3.3. Audio Feature Extractor

To extract rich features from audio data, we incorporated the Wav2Vec2 model into the AVAR-Net for audio data. It is a self-supervised model that employs a convolutional neural network and transformer architecture to extract comprehensive

and context-rich representations from anomalous audio data. Initially, the raw audio waveform is standardized to zero mean and unit variance. Then the waveform is processed by a feature extractor that consists of seven consecutive 1-dimensional convolution layers. Formally, the convolutional operation for the i-th layer is expressed as in Eq 2.

$$f^{(i)} = \text{GELU}\left(W^{(i)} * f^{(i-1)} + b^{(i)}\right) \tag{2}$$

Where $W^{(i)}$ and $b^{(i)}$ are learnable weights and biases, $f^{(i-1)}$ denotes the output from the preceding convolutional layers. Before employing GELU activation, the output of the first convolutional layer is group normalized, mathematically shown in Eq 3, to provide each of the 512-channel sequences with a zero mean and unit variance. The output of the subsequent convolutional layers is directly activated with GELU and does not include any normalizing layers.

$$f^{(i)} = \text{GELU}\left(\text{GroupNorm}\left(W^{(i)} * f^{(i-1)} + b^{(i)}\right)\right) \tag{3}$$

The feature extractor's output is a 512-dimensional encoded vector sequence. Each vector has a receptive field of 20 ms, which is comparable to the window sizes in spectral-based representations. After extracting features, each encoded anomaly vector representation in the sequence undergoes normalization to zero mean and unit variance before being projected into 768 dimensions by a single, shared, fully connected layer known as the feature projector. Dropout is then applied to all projections without any activation. The entire sequence is masked similarly to Spec Augment, where 0 or more random sets of consecutive vectors (masking in the time domain) and 0 or more random sets of consecutive channels (masking in the frequency domain) are set to 0. To create a relative positional embedding for each projected representation, the masked projected sequence is convolved by a single layer with a kernel size of 128, a stride of 1, padding of 64, 16 groups, and GELU activation. When the original convolutional input is added to this relative positional embedding, the receptive field is adjusted from 20 ms to 2.5 s. Lastly, dropout is applied after each vector has been independently normalized using Layer Norm. The resulting projected and masked sequence, enriched with positional and local context, is then processed by an encoder comprised of 12 consecutive transformer layers is fed with the projected and masked sequence alongside positional and local information. Each transformer layer consists of a residual 12-headed self-attention module and a residual 2-layer feed-forward network with 3072 and 768 units, respectively. Formally, the self-attention operation with residual connection is given by Eq 4.

$$H' = \text{LayerNorm}\left(H + \text{softmax}\left(\frac{QK^T}{\sqrt{d_k}}\right)V\right) \tag{4}$$

Where Q, K, and V denote queries, keys, and values, respectively, d_k denotes key dimensionality. The residual connection adds the input H to the attention output before normalization, ensuring training stability as expressed in Eq 5.

$$H'' = \text{LayerNorm}\left(H' + \text{FFN}(H')\right) \tag{5}$$

Where H' represents the output of the self-attention module. FFN is a feed-forward Network. The resulting output sequence is utilized in a downstream task, where each representation contains both local and global information due to self-attention.

3.4. Fusion Strategy

The visual and audio features are integrated using an early fusion strategy, wherein features from both modalities are concatenated at the feature level prior to input into the temporal model. This early integration facilitates the learning of cross-modal interactions, allowing the network to capture richer and more discriminative joint representations. Formally, given visual features $V \in \mathbb{R}^{T\times d_v}$ and audio features $A \in \mathbb{R}^{T\times d_a}$, the fused representation $F \in \mathbb{R}^{T\times(d_v+d_a)}$ is obtained by Eq 6. Where V, A represent video and audio features, respectively.

$$F = \text{Concat}(V, A) \tag{6}$$

3.5. Sequential Pattern Learning

Additionally, to capture long-range sequences in the data, we employed a Multi-stage Dilated TCN model on fused features. It consists of blocks, each containing a sequence of L convolutional layers. The activation at each layer and block has the same number of filters and follows a fixed dimension. Each layer consists of dilated convolutions with rate parameters, a non-linear function, and a residual connection. Dilated convolutions use a gap between filter elements, expanding the receptive field exponentially without increasing model depth, allowing the network to capture short and long-term patterns. Given feature sequence $x(t)$, a dilated convolution at time t is computed as in Eq 7.

$$Y(t) = \sum_{i=0}^{k-1} w_i \cdot x(t - d \cdot i) \tag{7}$$

Where $d = 2^l$ manages the dilation rate at the layer l. This ensures a progressively increasing receptive field. The result of the dilated convolution is processed by adding a residual connection to allow the model to learn incrementally and prevent information loss. The output of the residual block is computed in Eq 8.

$$S_t^{(j,l)} = S_t'^{(j,l)} + VS_t^{(j,l-1)} + e \tag{8}$$

Where V and e are the weights and biases of the residual, respectively. The receptive field at each step captures long-range dependencies, which are critical for anomaly recognition. The receptive field in MTCNs grows exponentially with several layers. Given B blocks and L layers per block, the total receptive field is as given by Eq 9.

$$r(B, L) = B \cdot 2^L \tag{9}$$

To highlight salient temporal features, an attention mechanism comprising a 1D-CNN followed by a self-attention module is incorporated. This combination captures both local and global dependencies, enhancing the model's ability to focus on informative steps before processing through the MTCN layers. The final feature is passed through a SoftMax function, which predicts the probabilities of different anomaly classes. The anomaly prediction at time t is given in Eq 10. Where U and c are learnable parameters.

$$Y_t' = \text{softmax}(UZ_t + c) \tag{10}$$

4. Experimental Result

This section outlines experimental setup, evaluation metrics, and datasets. It also presents the experimental results, both qualitative and quantitative, as well as the ablation study of the proposed framework. These are explained in the sections below.

4.1. Experimental setup

The experiments were conducted on a system equipped with an NVIDIA GTX 3090 Ti GPU and 32 GB of onboard memory. The experiments were implemented using the PyTorch framework in the Python programming language. The initial learning rate was set to 1×10^{-2} and dynamically adjusted to minimize the validation loss. Based on the experimental results, the final learning rate converged to 1×10^{-5}. Several experiments were conducted with different numbers of epochs, and the best results were obtained with 50 epochs across all datasets.

4.2. Evaluation metrics

The proposed framework is evaluated using several metrics, including accuracy (Acc), Precision (P), Recall (R), Average Precision (AP), and F1-score (F1). These are well-known metrics in the video classification domain that have been used by many researchers [48, 49]. To calculate these metrics, the numbers of true positives (TP), false positives (FP), true negatives (TN), and false negatives (FN) are determined. TP and FP represent the correctly and incorrectly classified positive samples, respectively. TN and FN are the numbers of correctly and incorrectly classified negative samples, respectively.

The Acc metric measures the model's performance in correctly classifying positive and negative classes, as given in Eq 11.

$$\text{Acc} = \frac{TP + TN}{TP + TN + FP + FN} \tag{11}$$

Precision is computed by dividing the total number of expected positives by the number of genuine positive predictions, as given in Eq 12.

$$\text{Precision} = \frac{TP}{TP + FP} \tag{12}$$

In contrast, Recall measures how well the model identifies all true positive instances out of the total positive instances, as given in Eq 13.

$$\text{Recall} = \frac{TP}{TP + FN} \tag{13}$$

The F1-score is a metric that combines Precision and Recall. This measure is calculated as the harmonic mean of the two metrics, as shown in Eq 14.

$$\text{F1 Score} = 2 \times \frac{\text{Precision} \times \text{Recall}}{\text{Precision} + \text{Recall}} \tag{14}$$

Finally, for understanding the trade-off between Precision and Recall, the Average Precision (AP) is a metric that evaluates the precision of a model at different recall levels, providing a single-figure summary of the precision-recall curve as provided in Eq 15.

$$AP = \sum_{n=1}^{N} (R_n - R_{n-1})\, P_n \tag{15}$$

Where R_n is the recall at threshold n, and P_n is the precision at threshold n.

4.3. Datasets

To evaluate the model's performance, this study utilized three datasets: (1) the publicly available *XD-Violence Detection* dataset, (2) a refined version referred to as *XD-Violence Recognition*, and (3) proposed *VAAR* dataset. The XD-Violence Detection dataset is commonly used for binary anomaly detection (normal vs. abnormal). XD-Violence Recognition builds upon this dataset, with refined annotations to support multi-class anomaly classification. The proposed dataset was specifically developed for this work and contains synchronized audio-visual data designed for robust real-world anomaly recognition. Each dataset is discussed in the section below.

4.3.1. XD-Violence

The dataset is a large-scale audio-visual benchmark for anomaly detection, compiled from real-world movies, web videos, sports broadcasting, and surveillance footage [19]. It consists of 4754 untrimmed film video clips, approximately 217 hours of footage. Each video has a video-level annotation in the training set and frame-level labels in the test set, making it well-suited for both weakly and strongly supervised tasks. *XD-Violence* is widely used in the literature for binary anomaly detection tasks (normal vs. abnormal). In this study, the dataset is extended to support recognition. It has six anomalous categories: abuse, car accidents, explosions, fighting, riots, and shootings. The dataset comprises a total of 1,912 videos, categorized into six anomaly classes: 49 videos depict abuse, 401 involve car accidents, 343 contain explosions, 417 show fighting, 372 represent riots, and 330 feature shootings. All videos are fully labeled, and the anomalous segments have been precisely identified based on the annotations provided.

4.3.2. The Proposed VAAR

In the field of anomaly recognition, the availability and quality of datasets remain a critical challenge, as most existing datasets are either not publicly accessible or contain only visual data. To address this limitation, the *VAAR* dataset is introduced as a curated benchmark designed to reflect diverse, real-world anomalous events across both visual and audio modalities. The curation of the dataset is discussed in Section 2.1. The curation was conducted in three stages by independent annotation teams. A clear labeling protocol was followed, wherein segments were carefully cropped to ensure that anomalous events were fully captured within each clip, minimizing unrelated or ambiguous content. The dataset also includes a dedicated "normal" class, composed of scenes with no anomalous activity. This enables the dataset to support both binary and multi-class anomaly recognition tasks. Each video was reviewed by multiple annotators, and inconsistencies were resolved through

Figure 2: Sample video frames from the same anomaly classes in the proposed dataset and XD-Violence, illustrating differences in visual context and anomaly depiction.

cross-validation among teams to enhance labeling reliability and reduce subjectivity. Initially, a wide range of anomaly categories was considered. Based on frequency and relevance in real-world surveillance, the annotation teams selected ten high-priority anomaly types. These categories have often been underrepresented in existing datasets, despite their significance in both public and private environments. The final release contains 300 clips per category, totaling 3,000 videos, ensuring balanced class distribution. Videos vary in resolution, with most captured at 720×1080 pixels, consistent with typical surveillance and mobile camera footage. Samples from the dataset are illustrated in Figure 2. In comparison to the *XD-Violence* dataset, the proposed *VAAR* dataset more accurately captures real-world scenarios, offering a richer and more realistic depiction of anomalous events as they commonly occur in everyday contexts. Additionally, to analyze the distribution of the proposed dataset, the visualization of its feature representations is illustrated in Figure 3.

4.4. Ablation Study

The section presents a comprehensive ablation study aimed at evaluating the effectiveness of the proposed method. Modality Features Analysis and Feature Fusion Strategies. The modality features analysis investigates the impact of different modalities on the overall performance of the method, with a series of experiments designed to assess how each modality contributes to the method's effectiveness. This analysis helps highlight the strengths and limitations of individual modalities. In the Feature Fusion Strategies section, various fusion techniques are tested to determine the most

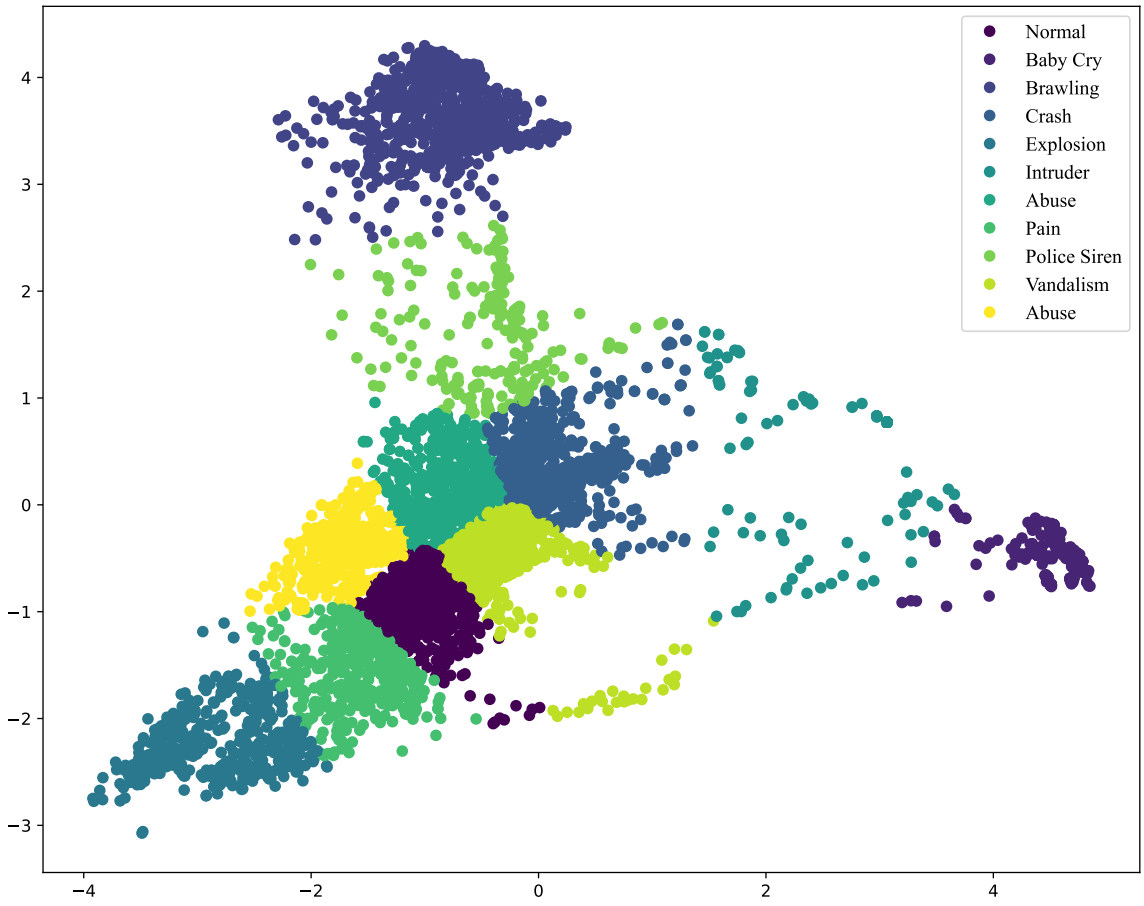

Figure 3: Feature visualization of the proposed dataset using dimensionality reduction, where high-dimensional audio-visual embeddings are projected into a 2D space. Each color corresponds to an anomaly class, showing distinct clustering patterns and inter-class relationship.

efficient way to combine the features from different modalities. By experimenting with different fusion strategies, this study assesses the effectiveness of each approach in improving the model's overall efficiency, providing a thorough evaluation of the fusion process, and further validating the superiority of the proposed method.

4.4.1. Modality Feature Analysis

This section outlines the experimental results of the *AVAR-Net* over the *VAAR* and *XD-Violence Recognition and Detection* datasets. Initially, the study conducted experiments utilizing only audio features for anomaly recognition. Subsequently, it examined the visual features for anomaly recognition, followed by experiments fus-

Table 2: Experimental results of the proposed framework compared with other sequential models for audio, video, and fused feature extraction on the VAAR and XD-Violence Recognition (XD-VR) datasets. Accuracy, Precision, Recall, and F1-Score are represented by Acc, Pre, Rec, and F1, respectively.

Dataset	**Models**	**Audio**				**Video**				**Fused**			
		Acc	Pre	Rec	F1	Acc	Pre	Rec	F1	Acc	Pre	Rec	F1
VAAR	GRU	12.81	09.34	12.80	08.83	53.52	51.02	53.52	50.24	65.06	63.65	65.06	63.53
	Bi-GRU	31.62	31.62	36.10	32.16	54.83	52.92	56.83	55.03	50.14	48.26	50.14	47.86
	LSTM	16.13	12.04	16.13	09.80	56.13	53.90	56.13	54.47	63.10	63.82	63.10	63.13
	Bi-LSTM	35.60	36.86	35.60	32.33	57.23	54.48	57.23	53.27	67.02	66.24	67.02	65.76
	Trans	60.00	61.40	60.00	60.50	64.13	55.40	64.00	59.00	67.03	66.04	57.03	65.48
	MTCN	**72.10**	**54.05**	**84.38**	**65.85**	**77.50**	**56.00**	**98.25**	**71.34**	**89.29**	**89.30**	**89.29**	**89.22**
XD-VR	GRU	25.06	14.76	25.06	18.50	65.45	63.79	65.45	64.38	63.13	63.21	63.13	62.11
	Bi-GRU	43.08	40.32	43.08	39.63	66.27	64.67	66.27	65.31	72.49	71.80	72.49	71.81
	LSTM	31.13	21.12	31.33	20.26	64.36	62.51	64.36	63.12	67.02	66.04	67.02	65.76
	Bi-LSTM	45.00	41.40	45.00	39.60	66.25	64.59	66.25	65.16	73.10	71.88	73.10	72.21
	Trans	50.00	46.00	50.00	48.40	68.25	68.78	68.25	66.89	74.00	69.00	74.00	70.20
	MTCN	**62.40**	**69.02**	**60.95**	**64.73**	**67.70**	**82.00**	**63.76**	**71.74**	**76.68**	**80.60**	**79.68**	**79.43**

ing audio-visual features for analysis. Afterward, the comparative analysis of the proposed framework with SOTA methods is performed, followed by the quantitative analysis, which evaluates the proposed framework results in different approaches. Finally, a detailed ablation study of the proposed framework is provided. We first evaluated *AVAR-Net* using only audio features extracted using the *Wav2Vec2* model. To assess temporal modelling capabilities, the study compared several sequential models, including GRU, Bi-GRU, LSTM, Bi-LSTM, Transformer, and the proposed MTCN. Performance was assessed on both the *VAAR* and *XD-Violence Recognition* datasets. From table 2, it can be seen that on the VAAR dataset, the GRU model performed the worst, achieving an accuracy of 12.81%, highlighting its difficulty in modeling complex audio dynamics. LSTM and Bi-LSTM improved modestly (16.13% and 35.60%, respectively), suggesting better but still limited capacity for temporal pattern recognition in audio-only settings. The Transformer performed significantly better, achieving 60.00% accuracy, likely due to its self-attention mechanism, which helps capture global context. However, it showed signs of training instability, possibly due to underfitting or its lack of inductive bias for temporal locality. The proposed MTCN model achieved the best performance at 72.10% accuracy, outperforming the transformer by 12.10%. This demonstrates MTCN's strength in modeling long-range dependencies efficiently through dilated convolutions and multi-stage design. On the *XD-Violence Recognition* dataset, the overall performance of all models decreased due to increased scene complexity and class imbalance. GRU, Bi-GRU, LSTM, and Bi-LSTM achieved 25.06%, 43.08%, 31.13%, and 45.00%, respectively. The Trans-

former reached 50.00%, while MTCN achieved the highest at 62.40%, offering a modest yet consistent improvement. These results suggest that MTCN generalizes more effectively across datasets than both recurrent and Transformer-based models in the audio-only setting. Next, the study evaluated the models using only video features extracted using the *MobileViT* model. Compared to audio, video generally carries richer contextual and spatial information, making it more informative for detecting complex activities. The study utilized MobileViT for video feature extraction and employed the same sequential models, including GRU, Bi-GRU, LSTM, Bi-LSTM, Transformer, and our proposed MTCN. Table 2 illustrates that on the VAAR dataset, GRU achieved an accuracy of 53.52%, with Bi-GRU, LSTM, and Bi-LSTM performing similarly at 52.92%, 53.90%, and 57.23%, respectively. These results highlight the limited ability of recurrent models to effectively capture long-range and non-linear temporal dependencies in complex visual data. The Transformer model performed notably better, achieving 64.13% accuracy, benefitting from its self-attention mechanism. However, it still struggled with fine-grained temporal modeling, likely due to a lack of inductive bias toward sequential ordering and reliance on positional encoding. Underfitting was also observed during training. The proposed MTCN model outperformed all other baselines, achieving 77.50% accuracy, a 13.37% absolute improvement over the Transformer. This result underscores MTCN's ability to model multi-scale temporal patterns using dilated convolutions and hierarchical block design, offering more robust and scalable video sequence analysis. On the *XD-Violence* dataset, a similar pattern emerged. Recurrent models again underperformed, with GRU, Bi-GRU, LSTM, and Bi-LSTM trailing behind. The Transformer reached 68.78% accuracy, while MTCN surpassed all models with a score of 82.00%, demonstrating strong generalization across datasets. These findings confirm that MTCN is more effective than both RNN-based and Transformer-based sequence models for modeling visual temporal patterns in surveillance data. However, despite its improvements, relying solely on video features still leaves performance gaps, especially in cases involving occlusion, poor lighting, or off-screen events. Finally, to assess the benefit of cross-modal integration, Experiments were conducted using fused audio and visual features. The audio features were extracted from the pre-trained *Wav2Vec2* model, and the video features were obtained from the pre-trained *MobileViT* model. These were combined using an early fusion strategy, where concatenated features were passed to each sequential model. Table 2 presents the performance of both datasets on the models. On the VAAR dataset, fusion consistently improved model performance compared to single-modality inputs. The GRU, LSTM, and Bi-LSTM achieved 65.06%, 63.10%, and 67.02% accuracy, respectively. The Transformer model performed notably better in the fused setting,

Table 3: Performance comparison of the proposed model with different sequence lengths on the VAAR and XD-Violence Recognition (XD-VR) dataset.

Dataset	Sequence Length	Accuracy (%)
VAAR	5	64.96
	15	84.37
	10	**89.29**
XD-VR	5	65.99
	15	71.65
	10	**76.68**

reaching 80.20% accuracy, showing a notable gain from modality fusion. However, the proposed MTCN model again achieved the best result, 82.42%, offering a modest 2.22% improvement over the Transformer baseline. On the *XD-Violence Recognition* dataset, similar to the VAAR dataset, the GRU, Bi-GRU, LSTM, Bi-LSTM, and Transformer models achieved accuracies of 63.13%, 65.31%, 63.12%, 65.16%, and 66.89%, respectively. The MTCN model achieved the highest accuracy of 76.68%, outperforming the Transformer by a significant margin. The consistent improvements across both datasets confirm that MTCN benefits more from fused inputs than other architectures. Its multi-stage temporal modeling and attention mechanism help to capture nuanced temporal dependencies in joint audio-visual sequences.

4.4.2. Features Fusion Analysis

To assess the design choices in *AVAR-Net*, the study conducted an ablation study focusing on two key factors: (1) the effect of sequence length on temporal modeling, and (2) the impact of fusion strategy on audio-visual integration. The effect of sequence length selection is investigated; sequence length determines how much temporal context is available to the model and plays a crucial role in capturing dynamic patterns. To identify the most suitable configuration, they study conducted a series of experiments with different sequence lengths: 5, 10, and 15. The result is shown in table 3. The model achieved the highest performance with a sequence length of 10, balancing sufficient context with manageable complexity. Shorter sequences (5) failed to capture long-range dependencies, while longer sequences (15) introduced noise and led to overfitting in some cases. Based on these findings, 10 frames were selected as the default for *AVAR-Net*, offering a strong trade-off between accuracy and generalization. Empirically, early fusion consistently outperformed late fusion

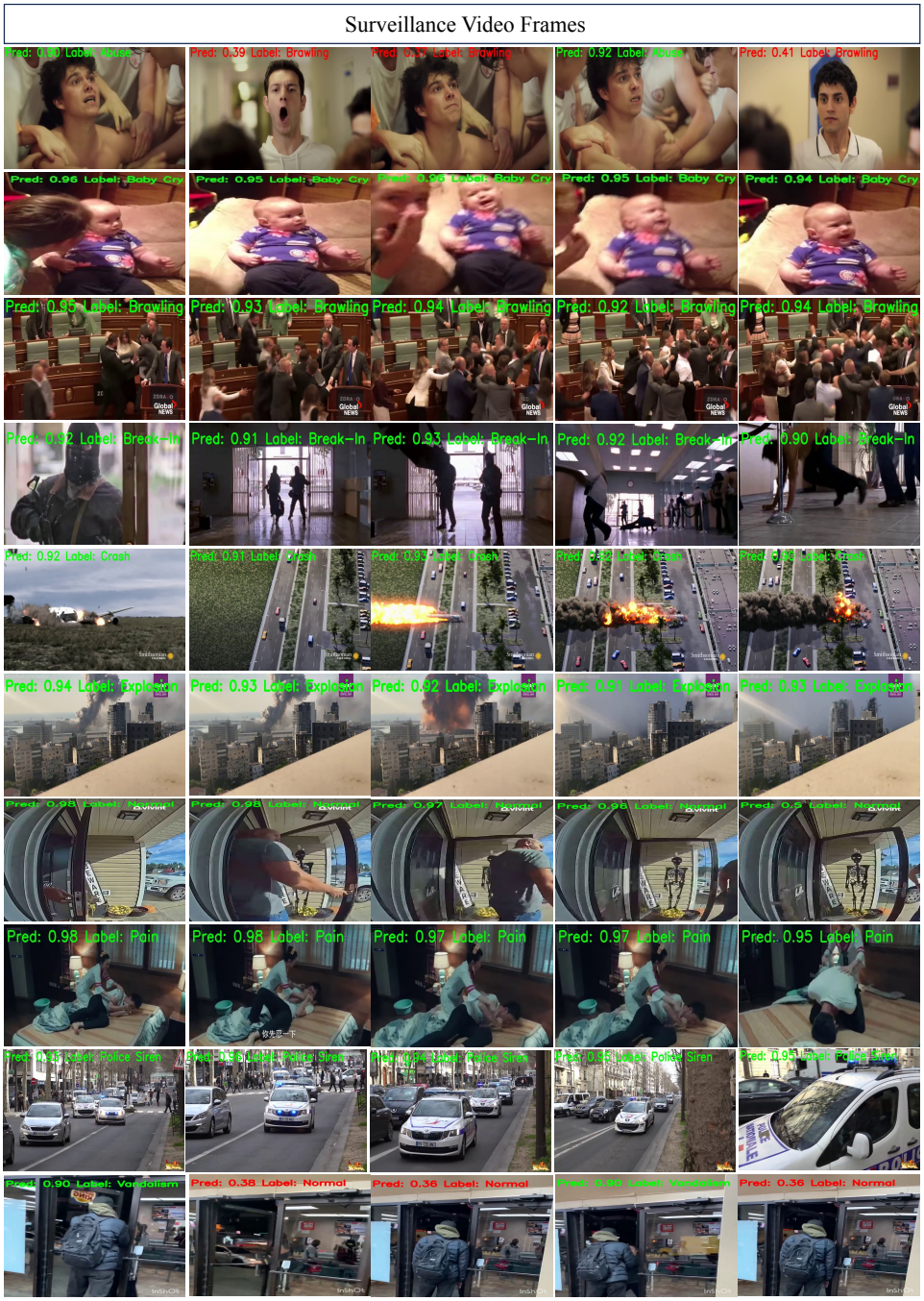

Figure 4: Visual analysis of AVAR-Net's predictions on challenging video samples from the proposed VAAR dataset. Each row corresponds to a video sequence, with individual frames labeled by their ground truth (GT) and model prediction.

Figure 5: The anomaly score curves for our proposed AVAR-Net model on both the XD-Violence Recognition (multi-class) and XD-Violence Detection (binary) datasets. The vertical axis shows the anomaly score, while the horizontal axis shows the number of frames with abnormal events. The anomaly scores are represented.

across both VAAR and XD-Violence datasets. On the VAAR dataset, early fusion achieved an accuracy of 89.29%, compared to 88.20% with late fusion. Similarly, on the XD-Violence Recognition dataset, early fusion reached 76.68%, outperforming late fusion at 75.05%. This improvement is likely due to the model's ability to learn joint feature representations earlier in the pipeline, allowing it to capture cross-modal correlations more effectively. Additionally, the number of parameters of the proposed model was 255,881 for the *VAAR* dataset and 86,985 for the *XD-Violence Recognition* dataset, overcoming the computational overhead. The study further confirms the effectiveness of early fusion in integrating audio and visual features.

4.5. Qualitative Analysis

A qualitative analysis was conducted to further assess the performance of the AVAR-Net, focusing on challenging cases from the VAAR dataset. For the visualization, the study conducted two different approaches: (1) frame-wise anomaly prediction visualization, and (2) anomaly score plots across video sequences. Figure 4 displays frame-level predictions for selected video clips. Each frame is labeled with the ground truth (GT) and predicted label (Pred). Incorrect predictions are highlighted in red, allowing for intuitive assessment of failure cases. The proposed model demonstrates strong performance in recognizing anomalies across a wide range of classes, even under difficult conditions such as occlusion, distant subjects, and overlapping actions. However, the AVAR-Net fails to correctly predict in certain complex cases, such as rows 1 and 10, which are colored red in Figure 4. Most of the video samples are correctly classified by our method despite the video posing certain challenges, distant activity from the camera viewpoint, overlapping actions, and complex scene composition. Despite these challenges, the proposed framework accurately recognized the anomalies. However, the proposed framework was confused by videos in the "Abuse" class, particularly distinguishing them from the "Brawling" class. In the first case, the second frame and the final frame are predicted as "Brawling" by the model. Although these frames do not visually depict brawling behavior, the presence of crowd noise in the accompanying audio likely contributed to the incorrect predictions. In contrast, the third frame presents visual activity that closely resembles brawling, specifically, the presence of a group of individuals in proximity, leading to further misclassification. Similarly, in the "Vandalism" video, the proposed framework failed to correctly identify the Normal class in the second, third, and final frames. These frames were misclassified as Normal due to the similarity of actions to typical normal behaviors, compounded by significant occlusion, where the key anomalous actions were partially or fully obscured by individuals in the scene. Additionally, the effectiveness of the proposed method was evaluated using anomaly scores evolving over video sequences. It is critical to note that the anomaly scores, represented by the blue lines in each figure, vary rapidly among abnormal classes and normal events. This pattern displays the AVAR-Net's ability to successfully discriminate rare abnormal events from the more common occurrences of regular events within a video. Figure 5 illustrates the fluctuation in the anomaly scores related to normal and different abnormal activities in the proposed *XD-Violence Detection* and *XD-Violence Recognition* datasets. For the *VAAR* dataset, Figure 5 (a) shows a group of people in the first frame, which is a normal frame, and the anomaly score is below 50%. In contrast, in the second frame, the brawling frames were similar to the Normal class. Additionally, the activity occurs when a group is fighting.

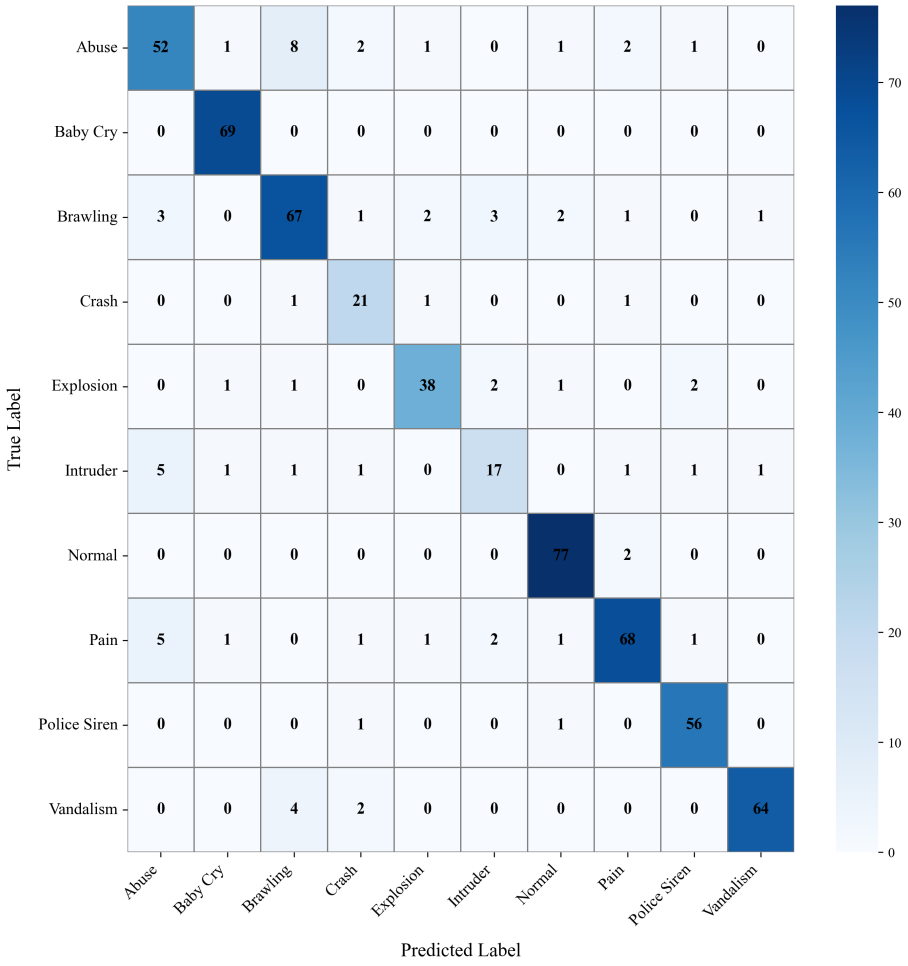

Figure 6: Confusion matrix of the proposed AVAR-Net model on the VAAR dataset.

The anomaly score jumps rapidly as the activity continues, and remains consistently high, and gradually decreases as the anomaly ends, as shown in the last frame. Similarly, Figure 5 (b) shows two pilots in the airplane, which is a normal frame, and the anomaly score is also lower. In the second and third frames, the plane crashes, and the anomaly score abruptly increases, indicating an anomaly in the frame. The anomaly remains high as it is in the frame, and the anomaly score decreases in the end when the anomaly finishes. For *XD-Violence Recognition*, Figure 5 (c) illustrates a car accident. The first shot depicts a man in a car, which is a normal event.

However, in the second frame, an unusual incident occurs when a car hits another

Table 4: Comparison of real-time performance metrics of proposed AVAR-Net on the proposed VAAR dataset

Dataset	FPS	Latency (ms)	Inference (ms)
VAAR	9.13	65.69	184.93

car. This abnormal act causes a significant increase in the anomaly score. Similarly, the third frame is a normal scene, and the anomaly score decreases gradually. Additionally, Figure 5 (d) depicts an anomaly event from the first frame showing the normal scene where a man with a gun appears in the frame. However, in the second frame, there is an abnormal event where a man is shooting. This scene caused a spike in the anomaly score, and finally, the last frame, which is a normal event where a man is jumping over a car, caused a significant decrease in the anomaly score. Additionally, a statistical analysis was performed on the proposed dataset, considering 100 video frames, to assess the generalization capability of AVAR-Net on the VAAR dataset. The corresponding results are presented in the table, where latency and inference time are measured in milliseconds. From the table, it can be seen that AVAR-Net exhibits low latency, demonstrating fast response and suitability for real-time processing. The corresponding inference time further indicates efficient computation and stable performance during video analysis on the VAAR dataset. Furthermore, the confusion matrix, as given figure 6, reveals that AVAR-Net achieves highly accurate recognition across most classes, with particularly strong performance for Normal (77 correct) and Baby Cry (69 correct) categories. Minor misclassifications occur between acoustically similar events such as Abuse and Brawling, indicating that the model effectively generalizes while maintaining robust class-wise discrimination. In the *XD-Violence Detection* dataset, Figure 5 (e) illustrates a normal event. In the first frame, a group of people is present in the frame, which is a normal event. Similarly, the second frame illustrates a normal event in which there is also a group of people. Thoroughly, in the video, the anomaly score remains under 50%. It remains constant, which demonstrates the accuracy and reliability of the proposed framework. Additionally, Figure 5 (f) depicts an instance of abnormal activity. In the first frame, a person is in the scene, which is considered a normal event. However, in the second frame, a fight scene between two men occurs, leading to a noticeable increase in the anomaly score, which remains constant as the fight continues, as shown in the third frame. Notably, there is a temporary decrease in the anomaly score observed during the moments of normal activity between the periods of elevated scores. Ultimately, the anomaly scores drop and return to baseline levels

Table 5: Comparative analysis of AVAR-Net with SOTA on the XD-Violence detection dataset using video-based modality, ordered by AP (%) from lowest to highest.

Method	**Backbone**	**AP (%)**
ZS (Video) [50]	-	25.36
ZS (Image) [50]	-	27.25
Hasan et al. [51]	-	31.25
LLAVA-1.5 [52]	-	50.26
LAVAD [53]	-	62.01
Wu et al. [19]	C3D-RGB	67.19
Wu et al. [19]	I3D-RGB	73.20
MSL [31]	-	75.53
Wu and Liu [54]	-	75.90
RTFM [55]	-	77.81
MSL [31]	-	78.28
Zhang et al. [56]	-	78.74
MSL [31]	VideoSwin-RGB	78.58
MGFN [57]	-	79.19
MGFN [57]	-	80.11
S3R [37]	-	80.26
Xu et al. [47]	I3D + Self-Attention	81.44
UR-DMU [56]	-	81.66
HyperVD [58]	-	82.51
AE-Net [36]	Adversarial	85.13
AVAR-Net	MobileViT	**86.54**

once the fight concludes.

4.6. Comparative Analysis

This section outlines the results of the proposed framework with other anomaly detection methods. The AVAR-Net is compared with state-of-the-art methods across different approaches, including semi-supervised methods [51, 61], training-free [52, 62, 50], and weakly supervised methods [19, 31, 36, 42, 43, 47, 54, 55, 63, 57]. Table 5 presents a visual comparison of the results with state-of-the-art methods; we carried out experiments on the *XD-Violence Detection* dataset. Notably, our method demonstrates superior performance compared to all the semi-supervised, training-free, and weakly supervised baselines, achieving a higher AP with a significant im-

Table 6: Comparative Analysis of AVAR-Net with SOTA on the XD-Violence detection dataset using visual-audio modality.

Methods	**Year**	**AP (%)**
Wu et al. [54]	2020	78.64
Wu et al.† [54]	2020	78.66
RTFM* [55]	2021	78.54
RTFM† [55]	2021	78.54
Pang et al. [10]	2021	81.69
MACIL-SD [59]	2022	83.40
UR-DMU [56]	2023	81.77
Zhang et al. [60]	2023	81.43
HyperVD [58]	2024	85.67
Leng et al. [42]	2024	87.61
Shin et al. [43]	2024	88.28
Xu et al. [47]	2025	84.06
AVCL [46]	2025	83.39
AVAR-Net	2025	**88.56**

provement of 24.53% AP, when compared to the LAVAD, which have the highest performance in the training free. Similarly, the proposed method achieved a significant minor improvement of 1.41% AP against the HyperVD [36] in a weakly supervised approach. Moreover, the existing methods utilize large models as extractors and classifier models. However, the proposed framework utilized a pre-trained *MobileViT*, which is lightweight as well as training-free, enabling it to be efficient for extraction while reducing the computational cost for real-time deployment. Similarly, for the visual-audio comparison, the study evaluated the results against the state-of-the-art methods as given in table 6. The proposed method leveraged dual modality on the *XD-Violence* dataset. Notably, our method demonstrates superior performance of 88.56% AP. The proposed method exhibited notable improvements

Table 7: Comparison of real-time performance metrics of AVAR-Net on the XD-Violence dataset.

Dataset	**FPS**	**Latency (ms)**	**Inference (ms)**
XD-Violence	4	112.23	429.87

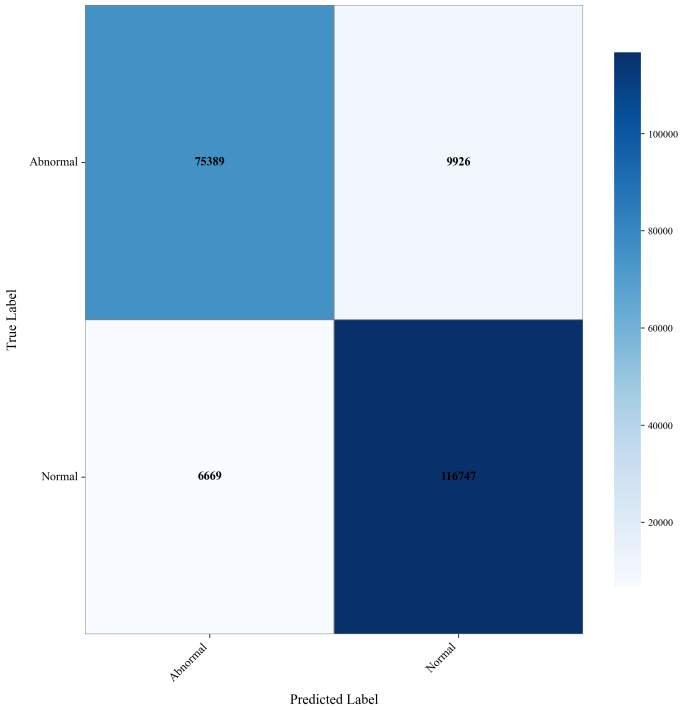

Figure 7: Confusion matrix of the proposed AVAR-Net model on the XD-Violence dataset.

in performance of 2.89%, 0.95%, and 0.28% AP when compared to the highest-performing methods, such as [58, 42, 43], as provided in table 6. The methods with † and ∗ are re-implemented and reported by [59]. From Table 4, it can be observed that AVAR-Net demonstrates strong real-time capability on the XD-Violence dataset, maintaining low inference and latency times that indicate efficient processing speed during testing. The consistently low uncertainty values reflect the model's confidence and stability. Furthermore, the confusion matrix illustrated in Figure 7 shows that AVAR-Net effectively differentiates between normal and abnormal events, with minimal misclassifications, demonstrating robust learning and accurate event recognition in complex real-world environments.

5. Conclusion and Future Work

In this study, a comprehensive audio-visual anomaly recognition approach was proposed to address the limitations of conventional systems that rely solely on visual information and often exhibit degraded performance under challenging real-world

conditions such as occlusion, low illumination, and off-screen events. The proposed approach combines a newly developed dataset with an efficient recognition framework. The VAAR dataset provides synchronized audio-visual recordings across ten diverse anomaly categories, serving as a valuable resource for advancing research in multimodal anomaly detection. In addition, the proposed AVAR-Net framework effectively integrates multimodal features extracted from both audio and visual sources using an early fusion mechanism. Specifically, MobileViT is employed to extract spatial and temporal visual representations from video frames, capturing both local and global scene information, while Wav2Vec2 processes raw audio waveforms to derive high-level temporal and spectral features that encode sound patterns associated with anomalous events. The fused audio-visual representations are then processed by a Multi-Stage Temporal Convolutional Network (MTCN), which models long-range temporal dependencies and enhances spatiotemporal reasoning for accurate anomaly recognition. Experimental evaluations on both the VAAR and XD-Violence benchmarks demonstrate that AVAR-Net achieves competitive performance, confirming its effectiveness and strong generalization capability across diverse real-world scenarios.

Beyond the reported results, this work builds the groundwork for advancing multimodal anomaly recognition in complex environments. Future efforts will focus on expanding the VAAR dataset to cover a wider range of real-world scenarios, developing adaptive fusion strategies for improved interpretability, and extending the framework to multi-view settings for greater robustness. We also plan to optimize AVAR-Net for real-time processing on edge devices, enabling efficient deployment in resource-constrained and time-critical surveillance applications.

Acknowledgments

This work was supported by the National Research Foundation of Korea (NRF), a grant funded by the Korea government (MSIT) , Grant/Award Number: (RS-2023-NR076686).

References

[1] Y. Chen, J. Li, E. Blasch, Q. Qu, Future outdoor safety monitoring: Integrating human activity recognition with the internet of physical–virtual things, Applied Sciences 15 (7) (2025) 3434.

[2] V. Tsakanikas, T. Dagiuklas, Video surveillance systems-current status and future trends, Computers & Electrical Engineering 70 (2018) 736–753.

[3] H. Xuan, Z. Zhang, S. Chen, J. Yang, Y. Yan, Cross-modal attention network for temporal inconsistent audio-visual event localization, in: Proceedings of the AAAI Conference on Artificial Intelligence, Vol. 34, 2020, pp. 279–286.

[4] S. Mo, Y. Tian, Multi-modal grouping network for weakly-supervised audio-visual video parsing, Advances in Neural Information Processing Systems 35 (2022) 34722–34733.

[5] S. Wang, Z. Miao, Anomaly detection in crowd scene, in: IEEE 10th International Conference on Signal Processing Proceedings, IEEE, 2010, pp. 1220–1223.

[6] C.-H. Demarty, C. Penet, M. Soleymani, G. Gravier, Vsd, a public dataset for the detection of violent scenes in movies: design, annotation, analysis and evaluation, Multimedia Tools and Applications 74 (17) (2015) 7379–7404.

[7] W. Liu, W. Luo, D. Lian, S. Gao, Future frame prediction for anomaly detection–a new baseline, in: Proceedings of the IEEE conference on computer vision and pattern recognition, 2018, pp. 6536–6545.

[8] W. Sultani, C. Chen, M. Shah, Real-world anomaly detection in surveillance videos, in: Proceedings of the IEEE conference on computer vision and pattern recognition, 2018, pp. 6479–6488.

[9] M. Perez, A. C. Kot, A. Rocha, Detection of real-world fights in surveillance videos, in: ICASSP 2019-2019 IEEE International Conference on Acoustics, Speech and Signal Processing (ICASSP), IEEE, 2019, pp. 2662–2666.

[10] W.-F. Pang, Q.-H. He, Y.-j. Hu, Y.-X. Li, Violence detection in videos based on fusing visual and audio information, in: ICASSP 2021-2021 IEEE international conference on acoustics, speech and signal processing (ICASSP), IEEE, 2021, pp. 2260–2264.

[11] D. C. Senadeera, X. Yang, D. Kollias, G. Slabaugh, Cue-net: violence detection video analytics with spatial cropping enhanced uniformerv2 and modified efficient additive attention, in: Proceedings of the IEEE/CVF Conference on Computer Vision and Pattern Recognition, 2024, pp. 4888–4897.

[12] M. Cheng, K. Cai, M. Li, Rwf-2000: An open large scale video database for violence detection, in: 2020 25th International conference on pattern recognition (ICPR), IEEE, 2021, pp. 4183–4190.

[13] O. Barkan, T. Reiss, J. Weill, O. Katz, R. Hirsch, I. Malkiel, N. Koenigstein, Efficient discovery and effective evaluation of visual perceptual similarity: A benchmark and beyond, in: Proceedings of the IEEE/CVF International Conference on Computer Vision, 2023, pp. 20007–20018.

[14] J. Gao, H. Yang, M. Gong, X. Li, Audio–visual representation learning for anomaly events detection in crowds, Neurocomputing 582 (2024) 127489.

[15] W. Ullah, A. Ullah, T. Hussain, K. Muhammad, A. A. Heidari, J. Del Ser, S. W. Baik, V. H. C. De Albuquerque, Artificial intelligence of things-assisted two-stream neural network for anomaly detection in surveillance big video data, Future Generation Computer Systems 129 (2022) 286–297.

[16] A. Abbasi, A. R. R. Javed, A. Yasin, Z. Jalil, N. Kryvinska, U. Tariq, A large-scale benchmark dataset for anomaly detection and rare event classification for audio forensics, IEEE Access 10 (2022) 38885–38894.

[17] E. Rushe, B. Mac Namee, Anomaly detection in raw audio using deep autoregressive networks, in: ICASSP 2019-2019 IEEE International Conference on Acoustics, Speech and Signal Processing (ICASSP), IEEE, 2019, pp. 3597–3601.

[18] A.-U. Rehman, H. S. Ullah, H. Farooq, M. S. Khan, T. Mahmood, H. O. A. Khan, Multi-modal anomaly detection by using audio and visual cues, IEEE Access 9 (2021) 30587–30603.

[19] P. Wu, J. Liu, Y. Shi, Y. Sun, F. Shao, Z. Wu, Z. Yang, Not only look, but also listen: Learning multimodal violence detection under weak supervision, in: European conference on computer vision, Springer, 2020, pp. 322–339.

[20] Y. Feng, Y. Yuan, X. Lu, Learning deep event models for crowd anomaly detection, Neurocomputing 219 (2017) 548–556.

[21] E. Bermejo Nievas, O. Deniz Suarez, G. Bueno García, R. Sukthankar, Violence detection in video using computer vision techniques, in: International conference on Computer analysis of images and patterns, Springer, 2011, pp. 332–339.

[22] T. Hassner, Y. Itcher, O. Kliper-Gross, Violent flows: Real-time detection of violent crowd behavior, in: 2012 IEEE computer society conference on computer vision and pattern recognition workshops, IEEE, 2012, pp. 1–6.

[23] W. Liang, J. Zhang, Y. Zhan, Weakly supervised video anomaly detection based on spatial–temporal feature fusion enhancement, Signal, Image and Video Processing 18 (2) (2024) 1111–1118.

[24] C. Lu, J. Shi, J. Jia, Abnormal event detection at 150 fps in matlab, in: Proceedings of the IEEE international conference on computer vision, 2013, pp. 2720–2727.

[25] A. Kaur, L. Kaur, Concealed weapon detection from images using sift and surf, in: 2016 Online International Conference on Green Engineering and Technologies (IC-GET), IEEE, 2016, pp. 1–8.

[26] S. Sudhakaran, O. Lanz, Learning to detect violent videos using convolutional long short-term memory, in: 2017 14th IEEE international conference on advanced video and signal based surveillance (AVSS), IEEE, 2017, pp. 1–6.

[27] A. Hanson, K. Pnvr, S. Krishnagopal, L. Davis, Bidirectional convolutional lstm for the detection of violence in videos, in: Proceedings of the European conference on computer vision (ECCV) workshops, 2018, pp. 0–0.

[28] B. Peixoto, B. Lavi, J. P. P. Martin, S. Avila, Z. Dias, A. Rocha, Toward subjective violence detection in videos, in: ICASSP 2019-2019 IEEE International Conference on Acoustics, Speech and Signal Processing (ICASSP), IEEE, 2019, pp. 8276–8280.

[29] A. Singh, D. Patil, S. Omkar, Eye in the sky: Real-time drone surveillance system (dss) for violent individuals identification using scatternet hybrid deep learning network, in: Proceedings of the IEEE conference on computer vision and pattern recognition workshops, 2018, pp. 1629–1637.

[30] S. S. Pereira, J. E. B. Maia, Mc-mil: video surveillance anomaly detection with multi-instance learning and multiple overlapped cameras, Neural Computing and Applications 36 (18) (2024) 10527–10543.

[31] S. Li, F. Liu, L. Jiao, Self-training multi-sequence learning with transformer for weakly supervised video anomaly detection, in: Proceedings of the AAAI Conference on Artificial Intelligence, Vol. 36, 2022, pp. 1395–1403.

[32] A. Vaswani, N. Shazeer, N. Parmar, J. Uszkoreit, L. Jones, A. N. Gomez, Ł. Kaiser, I. Polosukhin, Attention is all you need, Advances in neural information processing systems 30 (2017).

[33] P. Wu, X. Zhou, G. Pang, L. Zhou, Q. Yan, P. Wang, Y. Zhang, Vadclip: Adapting vision-language models for weakly supervised video anomaly detection, in: Proceedings of the AAAI Conference on Artificial Intelligence, Vol. 38, 2024, pp. 6074–6082.

[34] J. Cui, W. Liu, W. Xing, Crowd behaviors analysis and abnormal detection based on surveillance data, Journal of Visual Languages & Computing 25 (6) (2014) 628–636.

[35] B. Du, L. Ru, C. Wu, L. Zhang, Unsupervised deep slow feature analysis for change detection in multi-temporal remote sensing images, IEEE Transactions on Geoscience and Remote Sensing 57 (12) (2019) 9976–9992.

[36] X. Song, P. Liu, S. Li, S. Xu, K. Wang, Adversarial erasure network based on multi-instance learning for weakly supervised video anomaly detection, Neurocomputing 636 (2025) 130030.

[37] C. Feng, Z. Chen, A. Owens, Self-supervised video forensics by audio-visual anomaly detection, in: proceedings of the IEEE/CVF conference on computer vision and pattern recognition, 2023, pp. 10491–10503.

[38] P. Kumari, M. Saini, An adaptive framework for anomaly detection in time-series audio-visual data, IEEE Access 10 (2022) 36188–36199.

[39] A. Owens, J. Wu, J. H. McDermott, W. T. Freeman, A. Torralba, Ambient sound provides supervision for visual learning, in: European conference on computer vision, Springer, 2016, pp. 801–816.

[40] R. Arandjelovic, A. Zisserman, Look, listen and learn, in: Proceedings of the IEEE international conference on computer vision, 2017, pp. 609–617.

[41] J. Kittler, I. Kaloskampis, C. Zor, Y. Xu, Y. Hicks, W. Wang, Intelligent signal processing mechanisms for nuanced anomaly detection in action audio-visual data streams, in: 2018 IEEE International Conference on Acoustics, Speech and Signal Processing (ICASSP), IEEE, 2018, pp. 6563–6567.

[42] J. Leng, Z. Wu, M. Tan, Y. Liu, J. Gan, H. Chen, X. Gao, Beyond euclidean: Dual-space representation learning for weakly supervised video violence detection, Advances in Neural Information Processing Systems 37 (2024) 17373–17397.

[43] J. Shin, A. S. M. Miah, Y. Kaneko, N. Hassan, H.-S. Lee, S.-W. Jang, Multimodal attention-enhanced feature fusion-based weakly supervised anomaly violence detection, IEEE Open Journal of the Computer Society (2024).

[44] W.-C. Wang, S. De Coninck, S. Leroux, P. Simoens, Embedding-based pair generation for contrastive representation learning in audio-visual surveillance data, Frontiers in Robotics and AI 11 (2025) 1490718.

[45] C. Zhang, G. Li, Y. Qi, H. Ye, L. Qing, M.-H. Yang, Q. Huang, Dynamic erasing network with adaptive temporal modeling for weakly supervised video anomaly detection, IEEE Transactions on Neural Networks and Learning Systems (2025).

[46] J. Meng, H. Tian, G. Lin, J.-F. Hu, W.-S. Zheng, Audio-visual collaborative learning for weakly supervised video anomaly detection, IEEE Transactions on Multimedia (2025).

[47] C. Xu, C. Li, H. Xing, Discriminative score suppression for weakly supervised video anomaly detection, in: 2025 IEEE/CVF Winter Conference on Applications of Computer Vision (WACV), IEEE, 2025, pp. 9587–9596.

[48] A. Hussain, W. Ullah, N. Khan, Z. A. Khan, H. Yar, S. W. Baik, Class-incremental learning network for real-time anomaly recognition in surveillance environments, Pattern Recognition 170 (2026) 112064.

[49] A. Hussain, W. Ullah, N. Khan, Z. A. Khan, M. J. Kim, S. W. Baik, Tds-net: Transformer enhanced dual-stream network for video anomaly detection, Expert Systems with Applications 256 (2024) 124846.

[50] R. Girdhar, A. El-Nouby, Z. Liu, M. Singh, K. V. Alwala, A. Joulin, I. Misra, Imagebind: One embedding space to bind them all, in: Proceedings of the IEEE/CVF conference on computer vision and pattern recognition, 2023, pp. 15180–15190.

[51] M. Hasan, J. Choi, J. Neumann, A. K. Roy-Chowdhury, L. S. Davis, Learning temporal regularity in video sequences, in: Proceedings of the IEEE conference on computer vision and pattern recognition, 2016, pp. 733–742.

[52] H. Liu, C. Li, Y. Li, Y. J. Lee, Improved baselines with visual instruction tuning, in: Proceedings of the IEEE/CVF conference on computer vision and pattern recognition, 2024, pp. 26296–26306.

[53] L. Zanella, W. Menapace, M. Mancini, Y. Wang, E. Ricci, Harnessing large language models for training-free video anomaly detection, in: Proceedings of the IEEE/CVF Conference on Computer Vision and Pattern Recognition, 2024, pp. 18527–18536.

[54] P. Wu, J. Liu, Learning causal temporal relation and feature discrimination for anomaly detection, IEEE Transactions on Image Processing 30 (2021) 3513–3527.

[55] Y. Tian, G. Pang, Y. Chen, R. Singh, J. W. Verjans, G. Carneiro, Weakly-supervised video anomaly detection with robust temporal feature magnitude learning, in: Proceedings of the IEEE/CVF international conference on computer vision, 2021, pp. 4975–4986.

[56] H. Zhou, J. Yu, W. Yang, Dual memory units with uncertainty regulation for weakly supervised video anomaly detection, in: Proceedings of the AAAI Conference on Artificial Intelligence, Vol. 37, 2023, pp. 3769–3777.

[57] Y. Chen, Z. Liu, B. Zhang, W. Fok, X. Qi, Y.-C. Wu, Mgfn: Magnitude-contrastive glance-and-focus network for weakly-supervised video anomaly detection, in: Proceedings of the AAAI conference on artificial intelligence, Vol. 37, 2023, pp. 387–395.

[58] X. Peng, H. Wen, Y. Luo, X. Zhou, K. Yu, P. Yang, Z. Wu, Learning weakly supervised audio-visual violence detection in hyperbolic space, arXiv preprint arXiv:2305.18797 (2023).

[59] J. Yu, J. Liu, Y. Cheng, R. Feng, Y. Zhang, Modality-aware contrastive instance learning with self-distillation for weakly-supervised audio-visual violence detection, in: Proceedings of the 30th ACM international conference on multimedia, 2022, pp. 6278–6287.

[60] C. Zhang, G. Li, Y. Qi, S. Wang, L. Qing, Q. Huang, M.-H. Yang, Exploiting completeness and uncertainty of pseudo labels for weakly supervised video anomaly detection, in: Proceedings of the IEEE/CVF Conference on Computer Vision and Pattern Recognition, 2023, pp. 16271–16280.

[61] B. Schölkopf, R. C. Williamson, A. Smola, J. Shawe-Taylor, J. Platt, Support vector method for novelty detection, Advances in neural information processing systems 12 (1999).

[62] A. Radford, J. W. Kim, C. Hallacy, A. Ramesh, G. Goh, S. Agarwal, G. Sastry, A. Askell, P. Mishkin, J. Clark, et al., Learning transferable visual models from natural language supervision, in: International conference on machine learning, PmLR, 2021, pp. 8748–8763.

[63] J.-C. Wu, H.-Y. Hsieh, D.-J. Chen, C.-S. Fuh, T.-L. Liu, Self-supervised sparse representation for video anomaly detection, in: European Conference on Computer Vision, Springer, 2022, pp. 729–745.